Nonstabilizerness via Perfect Pauli Sampling of Matrix Product States

Guglielmo Lami[1] and Mario Collura[1,2]
[1]International School for Advanced Studies (SISSA), 34136 Trieste, Italy
[2]INFN Sezione di Trieste, 34136 Trieste, Italy

(Received 27 April 2023; accepted 5 October 2023; published 31 October 2023)

We introduce a novel approach to evaluate the nonstabilizerness of an N-qubits matrix product state (MPS) with bond dimension χ. In particular, we consider the recently introduced stabilizer Rényi entropies (SREs). We show that the exponentially hard evaluation of the SREs can be achieved by means of a simple perfect sampling of the many-body wave function over the Pauli string configurations. The sampling is achieved with a novel MPS technique, which enables us to compute each sample in an efficient way with a computational cost $O(N\chi^3)$. We benchmark our method over randomly generated magic states, as well as in the ground-state of the quantum Ising chain. Exploiting the extremely favorable scaling, we easily have access to the nonequilibrium dynamics of the SREs after a quantum quench.

DOI: 10.1103/PhysRevLett.131.180401

Introduction.—Quantum advantage [1,2] relies on harnessing a quantum system's exponential complexity to surpass classical computing limitations, potentially enabling efficient solutions to NP problems [3–5]. Entanglement is a fundamental feature accounting for this complexity, thus making necessary to exploit it proficiently in any quantum computation. Indeed, quantifying entanglement in many-body systems is a long-standing research focus, with various well-established measures, such as purity, entanglement entropy, negativity, and mutual information [6–9].

Nevertheless, entanglement is not the sole *resource* requiring quantification to discriminate between easy and hard to simulate quantum states. Indeed, several states despite encoding extensive entanglement can be efficiently simulated on a classical computer. These states are part of the *stabilizer states* [10], defined as quantum states exclusively achievable using Clifford unitaries from the computational basis state $|0\ldots0\rangle$ [11–16].

The Clifford group represents a class of unitary transformations that maps strings of Pauli operators over N qubits into other Pauli strings [15,17]. Because of this structure, stabilizer states can be compactly represented classically, and Clifford operations can be efficiently executed using this representation [11,12].

Therefore, to measure the hardness of simulating a quantum state, regardless its entanglement, it is essential to define a quantity that considers the amount of non-Clifford operations required for state preparation [18,19]. This quantity has been dubbed *nonstabilizerness* or *quantum magic*.

Several measures of nonstabilizerness have been proposed so far in quantum information theory [20–22], as for instance the robustness of magic [21]. Nevertheless they are typically hard to compute [23]. As a matter of fact, quantifying nonstabilizerness beyond a few qubits remains a major challenge. Recently the *stabilizer Rényi entropies* (SREs) were introduced in Ref. [24] as a possible way of quantifying the nonstabilizerness of a quantum state. However, since they depend on expectation values of all possible Pauli strings, computing SREs of a generic state is exponentially costly with the number of qubits. Nevertheless when the N-qubit state admits a matrix product state (MPS) representation with finite bond dimension χ, the SREs can be computed as the norm of a "$2n$ replica" MPS with effective bond dimension χ^{2n}, where n (integer) represents the Rényi index [25]. Unfortunately, such a norm can be computed at a cost $O(N\chi^{6n})$, thus having an unfavorable scaling with the bond dimension. For any practical purpose, this makes the approach unfeasible for $n > 2$ [26].

To overcome such limitations, we propose a new method which exploits the probabilistic nature of the SREs. The algorithm relies on a novel and efficient MPS sampling in the Pauli basis, reminiscent of some well-established MPS techniques [27,28]. The sampling is perfect since we directly obtain samples from the target probability distribution, without Markov chains. By sampling over $\mathcal{N}$ Pauli strings realizations, we are able to estimate the SREs with a computational cost scaling as $O(\mathcal{N}N\chi^3)$. We first benchmark our approach over a set of random realization of MPS states with large bond dimension. We then study the nonstabilizerness in the ground state of the quantum Ising chain, showing a prefect agreement with the free-fermions calculation. Finally, we use our method to compute for the first time the nonequilibrium dynamics of the SREs after a quench. We consider the Ising model with or without a longitudinal field and show how the confinement of the excitations [29], hugely affecting the entanglement dynamics, may play a role also in the time evolution of the SREs.

Preliminaries.—Let us consider a quantum system consisting of N qubits. We identify the Pauli matrices by $\{\sigma^\alpha\}_{\alpha=0}^3$, with $\sigma^0 = \mathbb{1}$, and with $\boldsymbol{\sigma} = \prod_{j=1}^N \sigma_j \in \mathcal{P}_N$ a generic N-qubits Pauli strings where $\mathcal{P}_N = \{\sigma^0, \sigma^1, \sigma^2, \sigma^3\}^{\otimes N}$. For a pure normalized state $\rho = |\psi\rangle\langle\psi|$, the SREs [24] are given by

$$M_n(\rho) = \frac{1}{1-n} \log \sum_{\boldsymbol{\sigma} \in \mathcal{P}_N} \frac{1}{2^N} \mathrm{Tr}[\rho\boldsymbol{\sigma}]^{2n}. \tag{1}$$

To understand the relation with usual Rényi entropies, one has to observe that the non-negative real-valued function $\Pi_\rho(\boldsymbol{\sigma}) = (1/2^N)\mathrm{Tr}[\rho\boldsymbol{\sigma}]^2$ sums to 1 [24], and therefore can be interpreted as a probability distribution on the set of Pauli strings. Thus $M_n(\rho) = (1-n)^{-1} \log \sum_{\boldsymbol{\sigma} \in \mathcal{P}_N} \Pi_\rho(\boldsymbol{\sigma})^n - N \log 2$, apart from a constant, does coincides with the n-Rényi entropy of the distribution $\Pi_\rho(\boldsymbol{\sigma})$, and it reduces to the Shannon entropy $M_1(\rho) = -\sum_{\boldsymbol{\sigma} \in \mathcal{P}_N} \Pi_\rho(\boldsymbol{\sigma}) \log \Pi_\rho(\boldsymbol{\sigma}) - N \log(2)$ for $n \to 1$. It has been shown that SREs have the following properties [24], accordingly, being a good measure of nonstabilizerness: (i) M_n vanishes for stabilizer states whereas is positive for other states; (ii) are invariant under Clifford unitaries; (iii) are additive. Moreover, they grow extensively with the system size N, thus making it possible to define nonstabilizerness density $m_n = M_n/N$ [25]. A violation of monotonicity for the SREs with $0 \leq n < 2$ has been reported for systems undergoing measurements in the computational basis [30].

Computing the SREs in Eq. (1) requires the evaluation of the expectation value of a generic power $\Pi_\rho(\boldsymbol{\sigma})^{n-1}$ [or $\log \Pi_\rho(\boldsymbol{\sigma})$ for $n = 1$] over the probability distribution $\Pi_\rho(\boldsymbol{\sigma})$ itself. This suggests a natural way to estimate the SREs, based on a sampling from $\Pi_\rho(\boldsymbol{\sigma})$.

Conditional sampling.—The task of sampling from the set of the Pauli strings $\boldsymbol{\sigma}$, which has size $D = 4^N$, may appear as exponentially hard. To overcome this difficulty, we rewrite the full probability in terms of conditional and prior (or marginal) probabilities as

$$\Pi_\rho(\boldsymbol{\sigma}) = \pi_\rho(\sigma_1)\pi_\rho(\sigma_2|\sigma_1)\cdots\pi_\rho(\sigma_N|\sigma_1\cdots\sigma_{N-1}), \tag{2}$$

where $\pi_\rho(\sigma_j|\sigma_1\cdots\sigma_{j-1}) = [\pi_\rho(\sigma_1\cdots\sigma_j)/\pi_\rho(\sigma_1\cdots\sigma_{j-1})]$ is the probability that the Pauli matrix σ_j occurs at position j given that the string $\sigma_1\cdots\sigma_{j-1}$ has already occurred at positions $1\ldots j-1$, no matter the occurrences in the rest of the system (i.e., marginaliing over all possible Pauli strings for the reaming qubits $j+1\ldots N$). Specifically, one has $\pi_\rho(\sigma_1\cdots\sigma_j) = \sum_{\boldsymbol{\sigma} \in \mathcal{P}_{N-j}} (1/2^N)\mathrm{Tr}[\rho\sigma_1\cdots\sigma_j\boldsymbol{\sigma}]^2$. In other terms, the conditional probability at the step j, i.e., $\pi_\rho(\sigma_j|\sigma_1\cdots\sigma_{j-1})$, can be thought as the probability $\pi_{\rho_{j-1}}(\sigma_j)$ of getting σ_j in the partially projected state

$$\rho_{j-1} \equiv \frac{\rho|_{\sigma_1\cdots\sigma_{j-1}}}{\pi_\rho(\sigma_1\cdots\sigma_{j-1})^{1/2}}, \tag{3}$$

where we have defined the state $\rho|_{\sigma_1\cdots\sigma_{j-1}} \equiv 2^{-N} \sum_{\boldsymbol{\sigma} \in \mathcal{P}_{N-j+1}} \times \mathrm{Tr}[\rho\sigma_1\cdots\sigma_{j-1}\boldsymbol{\sigma}]\sigma_1\cdots\sigma_{j-1}\boldsymbol{\sigma}$ where, in the Pauli matrices decomposition of ρ, we are only keeping the contribution with fixed $\sigma_1\cdots\sigma_{j-1}$. Notice that such state is not normalized, however $\mathrm{Tr}[\rho_{j-1}^2] = 1$, and the probability that the remaining string $\boldsymbol{\sigma} \in \mathcal{P}_{N-j+1}$ occurs is exactly given by $\pi_\rho(\boldsymbol{\sigma}|\sigma_1\cdots\sigma_{j-1})$. From the definition in Eq. (3), we can easily get the recursive relation $\rho_j = \pi_{\rho_{j-1}}(\sigma_j)^{-1/2}\rho_{j-1}|_{\sigma_j}$. Thanks to that, we can generate the outcomes (and the probabilities of that outcome) by iterating over each single qubit, and sampling each local Pauli matrix according to the conditional probabilities. Once a local outcome occurs, the state is updated accordingly, and the iteration proceeds until all qubits are sampled. At the end of this procedure, as a result of Eq. (2), we generated configurations $\boldsymbol{\sigma}$ with probability $\Pi_\rho(\boldsymbol{\sigma})$. In order for this method to be computationally affordable, we need an efficient way of (i) evaluating the conditional probabilities; (ii) updating the state according to the local outcome. In the following section we show that these conditions are met whenever the state admits a MPS representation.

MPS iterative algorithm.—We consider a pure state $|\psi\rangle$ represented in the MPS form [31–33] $|\psi\rangle = \sum_{s_1,s_2,\ldots,s_N} \mathbb{A}_1^{s_1}\mathbb{A}_2^{s_2}\cdots\mathbb{A}_N^{s_N}|s_1, s_2, \ldots, s_N\rangle$, with $\mathbb{A}_j^{s_j}$ being $\chi \times \chi$ matrices, except at the left (right) boundary, where $\mathbb{A}_1^{s_1}$ ($\mathbb{A}_N^{s_N}$) is a $1 \times \chi$ ($\chi \times 1$) row (column) vector. Here $|s_j\rangle \in \{|0\rangle, |1\rangle\}$ is a local computational basis. The state is assumed right normalized, namely, $\sum_{s_j} \mathbb{A}_j^{s_j}(\mathbb{A}_j^{s_j})^\dagger = \mathbb{1}$. Following the conditional sampling prescription described in the previous section, we start from the first term of the expansion in Eq. (2). This can be written as

$$\pi_\rho(\sigma_1) = \frac{1}{2^N} \sum_{\boldsymbol{\sigma} \in \mathcal{P}_{N-1}} \langle\psi|\sigma_1\boldsymbol{\sigma}|\psi\rangle\langle\psi^*|\sigma_1^*\boldsymbol{\sigma}^*|\psi^*\rangle, \tag{4}$$

where we used the fact that the Pauli matrices are Hermitian. In terms of the operators $\Lambda_{\sigma_i} = \frac{1}{2}\sigma_i \otimes \sigma_i^*$ and $\Lambda_i = \frac{1}{2}\sum_{\sigma_i}(\sigma_i \otimes \sigma_i^*)$, each acting on the local Hilbert space given by a spin and its replica, the previous equation reads $\pi_\rho(\sigma_1) = [\langle\psi| \otimes \langle\psi^*|]\Lambda_{\sigma_1}\Lambda_2\cdots\Lambda_N[|\psi\rangle \otimes |\psi^*\rangle]$. Now, the following property can easily be proven

$$[\langle s_i'| \otimes \langle r_i'|]\Lambda_i[|s_i\rangle \otimes |r_i\rangle] = \delta_{s_i',r_i'}\delta_{s_i,r_i}, \tag{5}$$

meaning that Λ_i is just two copies of the identity operator connecting the spin $|s_i\rangle$ and its replica (whose local computational basis is now indicated as $|r_i\rangle \in \{|0\rangle, |1\rangle\}$). Using Eq. (5) together with the right normalization of the

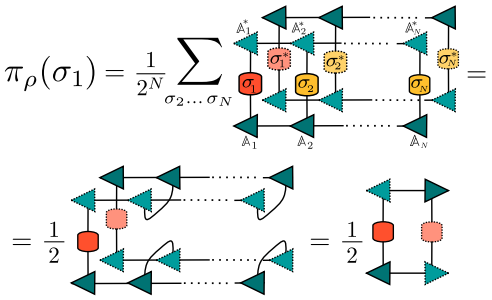

FIG. 1. MPS evaluation of the marginal probability $\pi_\rho(\sigma_1)$. Dotted lighter shapes represent conjugate tensors. Contractions over the auxiliary indices can be easily carried out thanks to the property in Eq. (5), together with the right normalization of the $\mathbb{A}_i$ tensors.

MPS, the computation of Eq. (4) reduces in the following local tensor contraction

$$\pi_\rho(\sigma_1) = \frac{1}{2} \sum_{s_1,s_1',r_1,r_1'} \left(\mathbb{A}_1^{s_1'}\right)^* \mathbb{A}_1^{r_1'}(\sigma_1)_{s_1' s_1} (\sigma_1^*)_{r_1' r_1} \mathbb{A}_1^{s_1} \left(\mathbb{A}_1^{r_1}\right)^*, \tag{6}$$

which is represented in Fig. 1 by means of the standard tensor network graphical notation [31,32].

After evaluating $\pi_\rho(\sigma_1)$ for $\sigma_1 \in \{\sigma^0, \sigma^1, \sigma^2, \sigma^3\}$, one can extract a sample from this distribution, obtaining the first element of the string. The information about the partially projected state Eq. (3) is encoded in an effective environment matrix $\mathbb{L} = [1/\sqrt{2\pi_\rho(\sigma_1)}] \sum_{s_1,s_1'} (\mathbb{A}_1^{s_1'})^*(\sigma_1)_{s_1' s_1} \mathbb{A}_1^{s_1}$. The calculation of the next terms of Eq. (2) and the extraction of the remaining σ_i proceeds following the same line. The full sampling recipe is summarized in the Algorithm 1, and graphically supported in Fig. 2. Extension of the Algorithm to mixed states is discussed in the Supplemental Material [34].

Sampling error.—We now discuss the statistical errors of the sampling algorithm, and their scaling with the system

Algorithm 1. Pauli sampling from MPS.

Input: a MPS $|\psi\rangle$ of size N

Put the MPS in right-normalized form.
Initialize $\mathbb{L} = (1)$ and $\Pi = 1$ [see Fig. 2(a)]
for $(i = 1,\ i = N,\ i++)$ **do**
  Compute the probabilities $\pi(\alpha) = \pi_\rho(\sigma^\alpha|\sigma_1 \cdots \sigma_{i-1})$ for $\alpha \in \{0,1,2,3\}$ as in Fig. 2(b).
  Generate a random value of α according to $\pi(\alpha)$
  Set $\sigma_i = \sigma^\alpha$, update $\Pi \to \Pi \cdot \pi(\alpha)$
  Update $\mathbb{L}$ as in Fig. 2(c).
end for

Output: a Pauli string $\boldsymbol{\sigma}$ and the probability $\Pi(\boldsymbol{\sigma})$

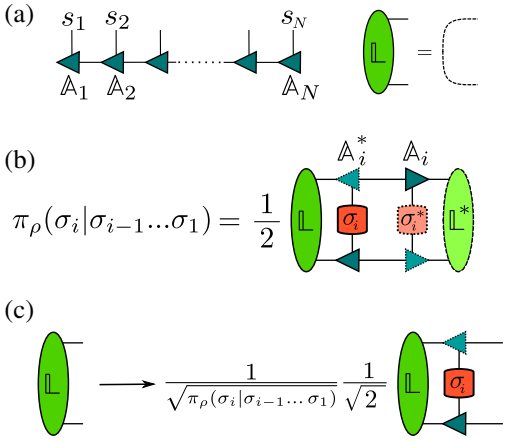

FIG. 2. The iterative sampling Algorithm 1.

size N. We first consider the case of estimating the n-SRE, with $n > 1$. As we saw, the estimation of $q_n = \sum_{\boldsymbol{\sigma} \in \mathcal{P}_N} \Pi_\rho(\boldsymbol{\sigma})^n$ is achieved by a statistical average over the samples $\{\boldsymbol{\sigma}_\mu\}_{\mu=1}^{\mathcal{N}}$, that means using the estimator $\tilde{q}_n = 1/\mathcal{N} \cdot \sum_{\mu=1}^{\mathcal{N}} \Pi_\rho(\boldsymbol{\sigma}_\mu)^{n-1}$. Afterwards, we evaluate the density of nonstabilizerness as $\tilde{m}_n = \big(N(1-n)\big)^{-1} \times \log \tilde{q}_n - \log 2$. Notice that $\tilde{q}_n$ is an unbiased estimator of q_n, since $\overline{\tilde{q}_n} = q_n$ [$\bar{\cdot}$ indicating the average over the uncorrelated samples, each distributed according to $\Pi_\rho(\boldsymbol{\sigma})$]. The fluctuations of $\tilde{q}_n$ are characterized by its variance, which can be easily evaluated as $\mathrm{Var}[\tilde{q}_n] = \mathrm{Var}[\Pi_\rho^{n-1}]/\mathcal{N}$. For every $n > 1$, one has $\mathrm{Var}[\Pi_\rho^{n-1}] < 1$ and thus we can upper bound the variance of the estimator obtaining $\mathrm{Var}[\tilde{q}_n] < \mathrm{const}/\mathcal{N}$, where const is a constant of $o(1)$, whose value is independent of the size $D = 4^N$ of the support of $\Pi_\rho(\boldsymbol{\sigma})$. This means that the statistical error on $\tilde{q}_n$ can be reduced arbitrarily by increasing the number of samples, no matter the system size N. However, since the uncertainty on $\tilde{m}_n$ propagates (at first order) as $\delta\tilde{m}_n \propto \delta\tilde{q}_n/\tilde{q}_n$ and both $\tilde{q}_n$, $\delta\tilde{q}_n$ are exponentially vanishing with N for typical probability distributions, $(\delta\tilde{m}_n)^2 \sim (1/\mathcal{N})\mathrm{Var}[\Pi_\rho^{n-1}]/(\overline{\Pi_\rho^{n-1}})^2$ is generally exponentially increasing with N [35]. Nevertheless, for the physical states we have examined, the estimation error $\delta\tilde{m}_n$ is always under control for reasonable values of $\mathcal{N}$ (see the next section and Supplemental Material [34] for further details). For $n = 1$ we evaluate $q_1 = \sum_{\boldsymbol{\sigma} \in \mathcal{P}_N} \Pi_\rho(\boldsymbol{\sigma}) \times \log \Pi_\rho(\boldsymbol{\sigma})$ via the estimator $\tilde{q}_1 = 1/\mathcal{N} \cdot \sum_{\mu=1}^{\mathcal{N}} \log \Pi_\rho(\boldsymbol{\sigma}_\mu)$. We have $\mathrm{Var}[\tilde{q}_1] = \mathrm{Var}[\log \Pi_\rho]/\mathcal{N}$ and thus we are interested in giving an upper bound for $\mathrm{Var}[\log \Pi_\rho]$. Several works, e.g., Ref. [8], establish that $\mathrm{Var}[\log \Pi_\rho] \leq \frac{1}{4}\log^2(D) + 1$. Thus, in our case, $\mathrm{Var}[\tilde{q}_1] \lesssim N^2 \log^2(2)/\mathcal{N}$ meaning that *in the worst scenario* the number of samples has to scale as N^2 to reach a given accuracy in the estimation.

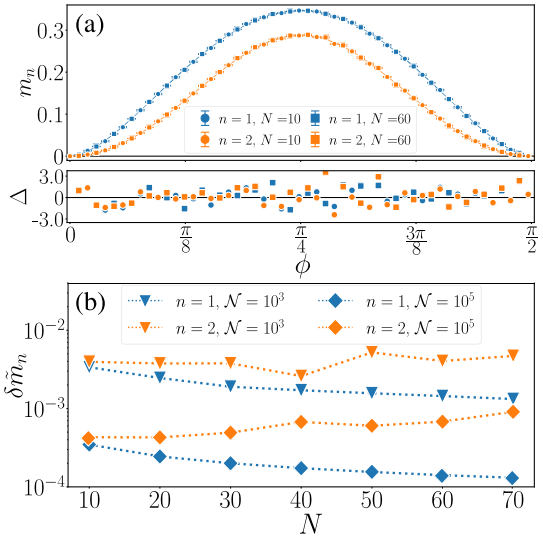

FIG. 3. (a) Density of nonstabilizerness of $|\psi\rangle = U_{\mathcal{C}}|T_\phi\rangle^{\otimes N}$ for $N = 10$, 60, $\mathcal{N} = 10^4$ and Rényi index $n = 1$, 2. In the lower strip we show the deviation from the analytical value $\Delta = (m_n - \tilde{m}_n)/\delta\tilde{m}_n$, $\tilde{m}_n$ being our estimation and $\delta\tilde{m}_n$ the propagated statistical error. (b) The error $\delta\tilde{m}_n$ as a function of the system size N for fixed $\mathcal{N} = 10^3, 10^5$, and $\phi \simeq \pi/4$.

Numerical experiments.—As a first benchmark of our algorithm, we consider the T state $|T_\phi\rangle = (|0\rangle + e^{i\phi}|1\rangle)/\sqrt{2}$, with ϕ ranging in $[0, \pi/2]$. A straightforward calculation yields to $M_2(|T_\phi\rangle\langle T_\phi|) = -\log[(1+\cos^4\phi + \sin^4\phi)/2]$, and $M_1(|T_\phi\rangle\langle T_\phi|) = -\cos^2\phi \times \log(|\cos\phi|) - \sin^2\phi \log(|\sin\phi|)$. Both quantities vanish for $\phi = 0, \pi/2$, while they have a maximum for $\phi = \pi/4$. We first initialize the system in the product state $|\psi_0\rangle = |T_\phi\rangle^{\otimes N}$, which is a MPS of bond dimension $\chi = 1$. Afterwards, we apply a random Clifford circuit $U_{\mathcal{C}}$ of depth N. In each layer, we randomly choose a sequence of one-qubit or two-qubit gates extracted from the generators $\{\mathbb{1}, S = \mathrm{diag}(1, i), H = (1/\sqrt{2})\left(\begin{smallmatrix}1 & 1\\ 1 & -1\end{smallmatrix}\right), \mathrm{CNOT}\}$ [17]. The final MPS $|\psi\rangle = U_{\mathcal{C}}|\psi_0\rangle$ has a larger bond dimension $\chi \gg 1$, whereas its nonstabilizerness is the same of $|\psi_0\rangle$, since this quantity is invariant under the Clifford group. Thanks to the additivity of the SREs, the nonstabilizerness density $m_n(|\psi\rangle) = M_n(|\psi\rangle)/N$ is equivalent to the nonstabilizerness of a single T state. We apply our sampling algorithm on $|\psi\rangle$, obtaining the estimation $\tilde{m}_n$. Results are shown in Fig. 3, for $n = 1$, 2 and size between $N = 10$ and $N = 70$. Notice that for $N = 70$, the bond dimension of $|\psi\rangle$ grows up to $\chi = 128$, depending on the particular arrangement of the Clifford layers. Values of χ of this order would be extremely challenging to target with previously known methods [25], whereas our approach takes only $\approx O(0.1)$ sec/sample on a single node simulation. Notice that the sampling can be easily parallelized, provided that the MPS is stored in multiple independent copies. All data points are in agreement with theoretical predictions within three error bars [see Fig. 3(a)]. Moreover, a scaling of the statistical error $\delta\tilde{m}_n$ with N at fixed value of $\mathcal{N}$ suggests that the fluctuations do not grow significantly with the system size, even though in principle we might have expected them to increase exponentially with N for $n = 2$.

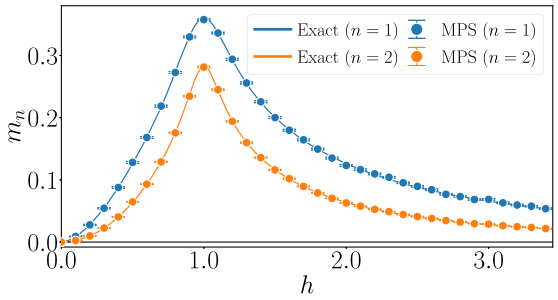

FIG. 4. Nonstabilizerness density of the Ising ground state ($g = 0$) with periodic boundary conditions, for a system of size $N = 14$ and Rényi index $n = 1$, 2. Exact results obtained in the free fermions representation [38] are compared with MPS sampling ($\mathcal{N} = 10^4$).

Afterwards, we consider the quantum Ising model $H = -\sum_i \sigma_i^x\sigma_{i+1}^x - h\sum_i \sigma_i^z - g\sum_i \sigma_i^x$. For $g = 0$, this Hamiltonian can be mapped into a model of free fermions [36,37], thus allowing the evaluation of the SREs in terms of $\sim 4^N$ determinants of matrices involving fermionic correlators [38]. In Fig. 4, we compare exact results for m_n ($n = 1, 2$) obtained in the fermionic representation with MPS estimations, for a system of size $N = 14$. For the MPS, we use the density matrix renormalization group (DMRG) [31] ($\chi = 32$) to find the ground state. MPS data are in perfect agreement with the exact values, within small error bars.

Finally, we use our algorithm to estimate the dynamics of the nonstabilizerness density during an out-of-equilibrium protocol. In particular, we prepare the system in the fully polarized state $|\psi(0)\rangle = |+\cdots+\rangle$, where $|+\rangle = (|0\rangle + |1\rangle)/\sqrt{2}$ is the eigenstate of σ^x with eigenvalue $+1$, and we consider the time evolution generated by the Ising Hamiltonian, i.e., $|\psi(t)\rangle = e^{-iHt}|\psi(0)\rangle$. We set the transverse and longitudinal fields, respectively, to $h = 0.5$ and $g = 0$, 0.25. The latter value corresponds to a phase in which the system is known to exhibit a dynamical confinement of the excitations [29,39], whereas in the free case ($g = 0$) the quasiparticles give rise to a light cone spreading of correlations [40]. We use the time evolving block decimation (TEBD) to compute the time evolution of the post-quench MPS [31,41], with bond dimension up to $\chi = 128$. Results are shown in Fig. 5 for $N = 40$. For $g = 0$, the nonstabilizerness density seems to saturate rapidly to a stationary value (see Ref. [42]), although the half-chain entanglement entropy $S = -\mathrm{Tr}[\varrho_{N/2}\log\varrho_{N/2}]$, is still growing linearly with the time t as expected (see the subplot). In the confined phase $g = 0.25$, nonstabilizerness exhibits large and persistent oscillations around a slightly

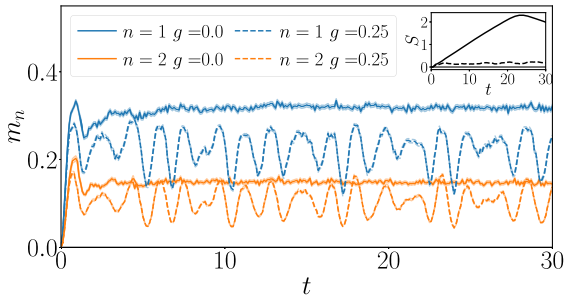

FIG. 5. Nonstabilizerness density after a quantum quench in the transverse and longitudinal field Ising model ($N = 40$). The system is prepared in the ferromagnetic state $|+\cdots+\rangle$ and quenched with parameters $h = 0.5$, $g = 0.0$ (solid line), $h = 0.5$, $g = 0.25$ (dotted line). The estimation is obtained with $\mathcal{N} = 10^3$ samples and pale lines represent the corresponding statistical uncertainty. Subplot: half-chain entanglement entropy.

lower stationary value, whereas entanglement is strongly suppressed and approaches a low saturation value. Oscillations of m_n are presumably linked to the presence of bound states consisting of pairs of domain walls (mesons). Indeed, we verified that the dominant frequencies of $m_n(t)$ are the same as those in the order parameter $\langle\sigma^x(t)\rangle$, thus representing the mesons masses [29].

Conclusions.—We have shown that a relatively new measure of quantum nonstabilizerness, the stabilizer Rényi entropies [24], can be estimated efficiently in the MPS framework via a perfect sampling of Pauli strings operators. Our estimation neither suffers from the exponential growth of the size of the many-body Hilbert space, nor shows an unfavorable scaling with the MPS bond dimension. As a matter of fact, we are able to consider either equilibrium or nonequilibrium wave functions with MPS bond dimension up to values that were out of reach by any of the previously proposed methods for evaluating the nonstabilizerness. Specifically, we applied our method to evaluate the amount of nonstabilizerness generated after a quench in the quantum Ising chain, and its sensitivity to the presence of confinement of excitations. Although we mainly focused on pure MPS, our algorithm can be easily adapted to nonpure states obtained from a MPS tracing out a subsystem consisting of the first or last qubits.

Our approach paves the way to novel numerical studies of the nonstabilizerness, possibly providing new characterizations of the quantum phases of matter, in and out of equilibrium. In addition, our new Pauli sampling technique for the MPS can be used to address crucial problems in quantum many-body theory, as, for instance, the operator scrambling.

Finally, we mention that an estimation of the SREs analogous to what we discussed is experimentally achievable in platforms enabling the preparation of duplicate states $|\psi\rangle \otimes |\psi\rangle$ and joint Bell basis measurements.

We thank Lorenzo Piroli for significant remarks on our manuscript and Alessandro Laio for useful suggestions about sampling strategies. We are particularly grateful to Titas Chanda, Marcello Dalmonte, Alioscia Hamma, and Emanuele Tirrito for collaborations on topics connected with this work, and for inspiring discussions. This work was supported by the PNRR MUR Project No. PE0000023-NQSTI (M. C.).

[1] J. Preskill, Quantum computing and the entanglement frontier, arXiv:1203.5813.
[2] J. Preskill, Quantum **2**, 79 (2018).
[3] R. P. Feynman, Int. J. Theor. Phys. **21**, 467 (1982).
[4] A. Y. Kitaev, A. H. Shen, and M. N. Vyalyi, *Classical and Quantum Computation*, Graduate Studies in Mathematics (American Mathematical Society, USA, 2002).
[5] P. Shor, in *Proceedings 35th Annual Symposium on Foundations of Computer Science* (IEEE Computer Society, 1994), pp. 124–134.
[6] L. Amico, R. Fazio, A. Osterloh, and V. Vedral, Rev. Mod. Phys. **80**, 517 (2008).
[7] P. Calabrese and J. Cardy, J. Stat. Mech. (2004) P06002.
[8] J. de Boer, J. Järvelä, and E. Keski-Vakkuri, Phys. Rev. D **99**, 066012 (2019).
[9] M. Dalmonte, V. Eisler, M. Falconi, and B. Vermersch, Ann. Phys. (Berlin) **534**, 2200064 (2022).
[10] D. Gottesman, Stabilizer Codes and Quantum Error Correction, arxiv:quant-ph/9705052.
[11] D. Gottesman, Phys. Rev. A **57**, 127 (1998).
[12] S. Aaronson and D. Gottesman, Phys. Rev. A **70**, 052328 (2004).
[13] H. J. García, I. L. Markov, and A. W. Cross, Quantum Inf. Comput. **14**, 683 (2014).
[14] S. Ball, A. Centelles, and F. Huber, Quantum error-correcting codes and their geometries, arXiv:2007.05992.
[15] D. Gottesman, arXiv:quant-ph/9807006.
[16] A. Kitaev, Ann. Phys. (Berlin) **303**, 2 (2003).
[17] M. A. Nielsen and I. L. Chuang, *Quantum Computation and Quantum Information: 10th Anniversary Edition* (Cambridge University Press, Cambridge, England, 2010).
[18] M. Howard, J. Wallman, V. Veitch, and J. Emerson, Nature (London) **510**, 351 (2014).
[19] J. R. Seddon, B. Regula, H. Pashayan, Y. Ouyang, and E. T. Campbell, PRX Quantum **2**, 010345 (2021).
[20] Z.-W. Liu and A. Winter, PRX Quantum **3**, 020333 (2022).
[21] M. Howard and E. Campbell, Phys. Rev. Lett. **118**, 090501 (2017).
[22] T. Haug and M. S. Kim, PRX Quantum **4**, 010301 (2023).
[23] M. Heinrich and D. Gross, Quantum **3**, 132 (2019).
[24] L. Leone, S. F. E. Oliviero, and A. Hamma, Phys. Rev. Lett. **128**, 050402 (2022).
[25] T. Haug and L. Piroli, Phys. Rev. B **107**, 035148 (2023).
[26] Only for $n = 2$, it is possible to exploit additional symmetries, further reducing the computational cost to $O(\chi^4)$.
[27] E. M. Stoudenmire and S. R. White, New J. Phys. **12**, 055026 (2010).
[28] A. J. Ferris and G. Vidal, Phys. Rev. B **85**, 165146 (2012).

[29] M. Kormos, M. Collura, G. Takács, and P. Calabrese, Nat. Phys. **13**, 246 (2016).
[30] T. Haug and L. Piroli, Quantum **7**, 1092 (2023).
[31] U. Schollwöck, Ann. Phys. (Amsterdam) **326**, 96 (2011).
[32] P. Silvi, F. Tschirsich, M. Gerster, J. Jünemann, D. Jaschke, M. Rizzi, and S. Montangero, *SciPost Physics Lecture Notes* (2019), 10.21468/scipostphyslectnotes.8.
[33] G. Vidal, Phys. Rev. Lett. **91**, 147902 (2003).
[34] See Supplemental Material at http://link.aps.org/supplemental/10.1103/PhysRevLett.131.180401 for additional information regarding our sampling techniques applied to mixed states. We also show some results concerning the sampling error and sampling from simple factorized states.
[35] This is because $\overline{\Pi_\rho^{2(n-1)}}/(\overline{\Pi_\rho^{n-1}})^2 \geq 1$.
[36] G. B. Mbeng, A. Russomanno, and G. E. Santoro, The quantum Ising chain for beginners, arXiv:2009.09208.
[37] P. Calabrese, F. H. L. Essler, and M. Fagotti, J. Stat. Mech. (2012) P07016.
[38] S. F. E. Oliviero, L. Leone, and A. Hamma, Phys. Rev. A **106**, 042426 (2022).
[39] N. Ranabhat and M. Collura, Thermalization of long range Ising model in different dynamical regimes: A full counting statistics approach, arXiv:2212.00533.
[40] P. Calabrese and J. Cardy, Phys. Rev. Lett. **96**, 136801 (2006).
[41] G. Vidal, Phys. Rev. Lett. **93**, 040502 (2004).
[42] D. Rattacaso, L. Leone, S. F. E. Oliviero, and A. Hamma, arXiv:2304.13768.